A R C H I V E S O F M E T A L L U R G Y A N D M A T E R I A L S
Volume 52 2007 Issue 2

A. BOKOTA*, T. DOMAŃSKI*

NUMERICAL ANALYSIS OF THERMO-MECHANICAL PHENOMENA OF HARDENING PROCESS OF ELEMENTS MADE OF CARBON STEEL C80U

ANALIZA NUMERYCZNA ZJAWISK TERMOMECHANICZNYCH PROCESU HARTOWANIA ELEMENTÓW WYKONYWANYCH Z WĘGLOWEJ STALI C80U

The work concerns numerical analysis of thermal phenomena, phase transformations and mechanical phenomena associated with hardening of carbon steel C80U. The following transformations were assumed: initial structure – austenite, austenite – perlite, bainite and austenite – martensite. Numerical algorithms for evaluation of fractions of phases and their kinetics based on continuous heating and cooling diagrams (CCT) were worked out. In the algorithm of thermal phenomena relation of thermophysical values to temperature and source of phase transformations were taken into account. The dilatometric tests on the simulator of thermal cycles were performed, during which the hardening of the elements made of carbon steel C80U was simulated. The results of dilatometric tests were compared with the results of the test numerical simulations. In this way the derived models for evaluating phase content and kinetics of transformations in heating and cooling processes were verified. The stresses generated during hardening were assumed to result from thermal load, structural plastic deformations and transformation plasticity. The hardened material was assumed to be elastic-plastic, and in order to mark plastic strains the non-isothermal plastic law of flow with the isotropic strengthening and condition plasticity of Huber-Misses were used. Thermophysical properties present in the model of mechanical phenomena were made dependant on both the phase composition and on temperatures. The results of numerical simulations confirm correctness of the algorithms that were worked out.

Praca dotyczy analizy numerycznej zjawisk cieplnych, przemian fazowych i zjawisk mechanicznych towarzyszących hartowaniu węglowej stali C80U. Założono istnienie przemian: struktura wyjściowa – austenit, austenit – perlit, bainit oraz austenit – martenzyt. Opracowano algorytmy numeryczne szacowania ułamków faz oraz ich kinetyki oparte na wykresach ciągłego nagrzewania oraz ciągłego chłodzenia (CTP_c). W algorytmie zjawisk cieplnych uwzględniono zależność wielkości termofizycznych od temperatury oraz źródła przemian fazowych. W celu zweryfikowania modelu szacowania udziałów fazowych i kinetyki przemian w procesach nagrzewania i chłodzenia wykonano badania dylatometryczne na symulatorze cykli cieplnych, podczas których symulowano hartowanie elementów wykonanych ze stali C80U. Wyniki badań dylatometrycznych porównano z wynikami symulacji numerycznej. Przyjęto, że naprężenia generujące się podczas hartowania są wynikiem obciążenia termicznego, odkształceń strukturalnych, plastycznych i odkształceń transformacyjnych. Założono, że hartowany materiał jest sprężysto-plastyczny, a do wyznaczania odkształceń plastycznych zastosowano prawo nieizotermicznego plastycznego płynięcia ze wzmocnieniem izotropowym i warunkiem plastyczności Hubera-Misesa. Wielkości termofizyczne występujące w modelu zjawisk mechanicznych uzależniono zarówno od składu fazowego jak i od temperatury. Wyniki symulacji numerycznych potwierdzają poprawność opracowanych algorytmów.

1. Introduction

The numerical modelling of the heat-treatment process, and then its simulation and control, requires many phenomena concurrent to such process to be taken into account. The correct prediction of the final proprieties is possible after defining the type and the property of the nascent microstructure of the steel- element in the process of heating, and then the cooling treated thermally. It is essential for the correct prediction of the final properties to define the type and the property of the microstructure formed in the process of heating, and then cooling of the heat treated steel-element. To achieve this, it is necessary to establish equations describing: fields of temperature, phase transformations in the solid state, as well as strains and stresses generated during the heat-treatment [1–6].

In the past the kinetics of phase transformations was determined only by curves of the cooling and a suitable

* INSTITUTE OF MECHANICS AND MACHINE DESIGN, CZESTOCHOWA UNIVERSITY OF TECHNOLOGY, 42-200 CZĘSTOCHOWA, 73 ST. DĄBROWSKIEGO STR., POLAND

transformations graph. Subsequently the kinetics determined stress distributions. At present the simulation of this phenomenon, based on the theory of the nucleation and the growth of grains, also involves transformation strains and heat sources of phase transformations are taken into account when modelling thermal phenomena [7]. The accuracy figure of the calculation of residual stresses during hardening depends on how precise the computer calculations of the temperature fields are.

Nowadays models of heat-treatment processes (hardenings) are being developed to include similar phenomena in processes of hot forming, such as: forging, rolling, welding etc. [8–12].

In many models, the coefficient of surface film conductance from hardened element surface was acknowledged as constant, or accepted as the linear function of temperature. In reality it is a non-linear function of temperature and surface quality [4, 5].

In numerical simulations of hardening processes of steel it is required to include transformation plasticity in models. This phenomenon causes irregular plastic flow of metals which takes place during phase transformations in the solid state [4, 13–15].

The last decade saw strong evolution of numerical methods whose aim to a greater or smaller extent was to design processes of heat-treatment. Every work dealing with this topic should contain thermal, microstructural and stress analysis. To implement this type of algorithms one usually applies the FEM which makes it possible to take into account both nonlinearities and inhomogeneity of thermally processed material. Special emphasis put on the development of this branch of numerical methods is inspired by the industry, which demands tools improving heat-treatment processes because of modern technologies and costs reduction trends [10, 16, 17].

On the basis of the current state of knowledge on hardening and data on mathematical and numerical modelling of heat-treatment phenomena, particularly - hardening, a complex model of hardening of the shallow-hardening tool steel was designed. The model includes thermal phenomena, phase transformations and mechanical phenomena. The designed computer programme enables hardening simulation of this steel as well as of steel with a similar chemical composition.

2. Phase transformations in hardened tool carbon steel

An array of different mathematical models was created after an analysis of received results. The elementary unit of almost all studies concerning transformations of the austenite into the ferrite, the pearlite and the bainite, is the Avrami equation [1, 14] for models based on TTT graphs and generalised Kolmogorow, Johnson-Mehl and Avrami equation for models using the classical theory of the nucleation [11, 13]. Whereas the fundamental equation for the austenite-martensite transformation is the Koisitenen and Marburger equation [4, 13, 18].

The choice of the suitable model may depend on the manner in which the hardening simulation is carried out. This can be the parallel simulation of thermal phenomena, phase transformations and mechanical phenomena or block- simulation arranged in rows – the thermal block, the block of phase transformations, and then the block of mechanical phenomena [5].

One ought to underline that in the block- simulation arranged in rows it is impossible to take into account the influence of the phase transformation heat on changes in temperature, both in the process of heating and cooling. This phenomenon is of little importance in the process of heating, however in the process of cooling (especially during the volumetric hardening) one noticed a significant influence of the phase transformation heat on changes in temperature within the range of the pearlite transformation existence [1, 7].

In the model of phase transformations graphs of continuous heating (CHT) and cooling (CCT) are used [19]. The phase fraction transformed during continuous heating (austenite) is calculated in the model using the Johnson-Mehl and Avrami formula:

$$\underline{\eta}_{\gamma}(T,t) = \sum \eta_{fp}\left(1 - \exp(-b\left(t_s, t_f\right)(t\,(T))^{n\left(t_s,t_f\right)}\right), \tag{2.1}$$

where: $b(t_s, t_f)$ and $n(t_s, t_f)$ are coefficients calculated assuming the initial fraction ((η_s) and the final fraction (η_f)), while η_{fp} is a sum of fractions of the initial structure phases (most often it is a ferrite-pearlite or pearlite structure, and $\sum \eta_{fp} = 1$).

Coefficients b and n are calculated using the formula (2.1) and on condition that the part of the nascent phase equals "η_s" during "t_s" and "η_f" in time "t_f". Formulas for these coefficients have a form:

$$n\left(t_s, t_f\right) = \frac{\ln\left(\ln\left(\eta_s\right)/\ln\left(\eta_f\right)\right)}{\ln\left(t_f/t_s\right)}, b\left(t_s, t_f\right) = \frac{-\ln\left(\eta_f\right)}{(t_s)^n}, \tag{2.2}$$

where: $t_s = t_s(T_s)$, $t_f = t_f(T_f)$, $\eta_s = 0.01$, $\eta_f = 0.99$, from the assumption.

The phase fraction during cooling, i.e. the ferrite or cementite fraction, the pearlite fraction or the bainite fraction are calculated using the formula:

$$\eta_{(\cdot)}(T,t) = \beta\left(1 - \exp\left(-b\left(t(T)\right)^n\right)\right),$$
$$\beta = \begin{cases} \eta^{\%}_{(\cdot)}\underline{\eta}_{\gamma} & \text{for } \underline{\eta}_{\gamma} \geqslant \eta^{\%}_{(\cdot)} \\ \underline{\eta}_{\gamma} & \text{for } \underline{\eta}_{\gamma} \leqslant \eta^{\%}_{(\cdot)} \end{cases}, \underline{\eta}_{\gamma} - \sum_k \eta_k \geqslant 0, \tag{2.3}$$

where: $\eta^{\%}_{(\cdot)}$ is the maximum phase fraction for the established of the cooling rate, estimated on the ground of the continuous cooling graph, $\underline{\eta}_{\gamma}$ is the fraction of austenite created in the process of heating, and $\sum_k \eta_k$ denotes the sum of fractions of phases created earlier in the cooling process.

The fraction of the martensite formed below the temperature M_s, is calculated using the Koistinen and Marburger formula [1, 18]:

$$\eta_M(T) = \beta\left(1 - \exp\left(-k(M_s - T)^m\right)\right),$$
$$k = -\frac{\ln\left(\eta_M^{\min} = 0.1\right)}{M_s - M_f}, \tag{2.4}$$

where: m is the constant chosen by means of experiment; for examined steels it is accepted that $m = 1$, whereas the constant "k" is calculated based on the condition that the transformation finishes at the temperature M_f, β is defined in (2.3).

For steel C80U for which $M_s \approx 240°C, M_f \approx -60°C$, the constant k equals: $k \approx 0.008$. This coefficient is comparable with the coefficient presented in literature as empirical ($c \approx 0.01$) for near-eutectoid carbon steels [4, 14].

2.1. The experiment and the verification of the model

The purpose of the dilatometric research was to analyse phase transformations during heating and continuous cooling of steel C80U, undergoing quick heating and then cooling at different rates. Dilatometric research was done in the Institute for Ferrous Metallurgy in Gliwice by means of a dilatometer DIL805 produced by Bähr Thermoanalyse GmbH. The dilatometer was equipped with a measuring- head of LVDT type, of theoretical resolution: ±0.057 μm. Temporary temperature deviations from a given value did not exceed ±0.5°C.

During the research critical temperatures A_{C1} and Ac_{cm} at fast heating (100°C/s) were defined. Also austenite phase transformations of the examined steel during simulated cycles of cooling (construction of the CCT graph) were studied. The error of a single result of the conversion temperature estimation did not exceed ±5°C. Particular components of the examined steel: 0.84C, 0.19Mn, 0.21Si, 0.006P, 0.003S, 0.11Cr, 0.08Ni, 0.03Mo, and 0.14Cu (%) remain within the range of admissible values defined by a suitable standard (PN-85/H-93002). Cylindrical samples ϕ4/2×10 mm and ϕ4/3×10 mm (for the velocity of cooling ⩾50°C/s) were used.

Heating to austenization temperature (1100°C) was carried out in the vacuum (pressure $<1\times10^{-4}$ mbar) with the velocity of 100°C/s, the heating (the austenization time) equaled 2 seconds (the same for all samples); the cooling of samples was carried out at different rate, established at.: 300, 200, 150, 100, 50, 30, 20 and 10°C/s.

For the established heating rate the temperatures of the beginning (A_{C1}) and the end of austenization (Ac_{cm}) were equal: 784 and 852±4°C respectively, whereas equilibrium temperatures Ac_1 and Ac_{cm} for this steel equal ~740 and ~760°C respectively [5, 19, 20].

After dilatometric tests the examination of the microstructure of samples, and measurement of their microhardness were carried out. Microsections of cross-sections of samples (in the half of their length) were etched with nital. The microstructures were observed and the pictures were recorded by means of the optical microscope Axiovet 25, manufactured by Zeiss, and a digital camera. A short description of the obtained microstructures of the steel C80U depending on the rate of cooling and their average hardness are given in the Table 1.

Using temperature curves, diagrams of individual dilatometric tests, fraction phases were assessed based on the examination of microstructures (figs. 10 and 11), and measurements of the microhardness, (tab. 1), the CCT graph of steel C80U was constructed (fig. 1). Basing on this graph, as well as on the CCT graph of steel C80U found in literature [19], the CCT graph was shifted so that it could be used for numerical simulation of phase fraction and phase kinetics (fig. 1). The graph shift results from the assumption present in the numeric algorithm that the calculation of the cooling process begins at the point when the temperature $T(t_{cool=0})$ = 810°C (1083 K) (While calculating the phase fraction the time of the cooling is counted from the moment of the intersection of the temperature curve of the cooling with a line T = 810°C, i.e it is assumed that time $t_{cool=0}$ at the moment of the intersection). This assumption was made on the basis of literature data [19].

In order to verify the model of phase transformations test- numerical simulations were carried out. Results of these simulations and appropriate comparisons to the experiment results are presented in pictures 2–5.

TABLE 1

Average microhardness and observed microstructures depending on the cooling rate

V_{cool}	Microhardness	Critical temperatures, °C					Observed microstructure
°C/s	HV 0.04	M_s	B_s	B_f	P_s	P_f	
10	370				670	612	pearlite- residual cementite
20	373				665	589	pearlite- residual cementite
30	416	241			640	545	pearlite- residual cementite
100	1055	235	308		608	424	martensite- residual bainite -retained austenite
200	1050	230	295		480	380	acicular martensite- residual bainite-retained aust.
300	1101	230			572	469	acicular martensite-retained austenite

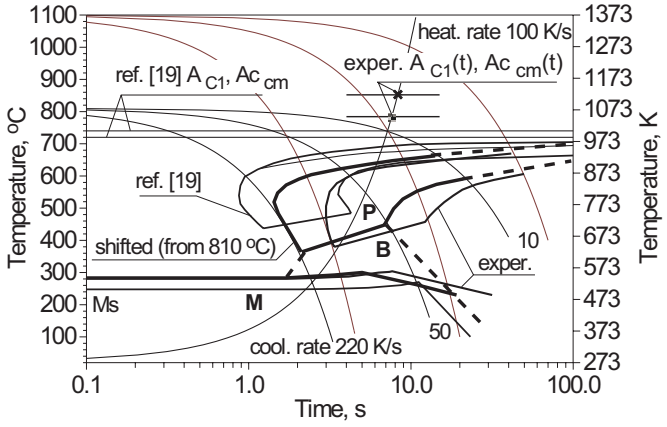

Fig. 1. The Time-Temperature-Transformation graph (CCT) for steel C80U and the shifted graph

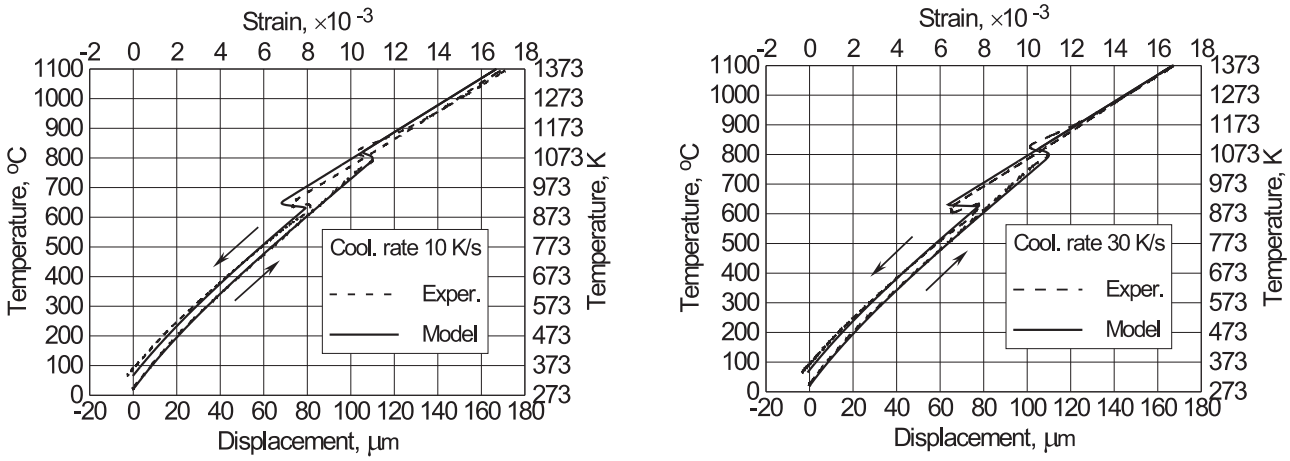

Fig. 2. Experimental and simulated dilatometric curves, cooling rate: a) 10 K/s, b) 30 K/s

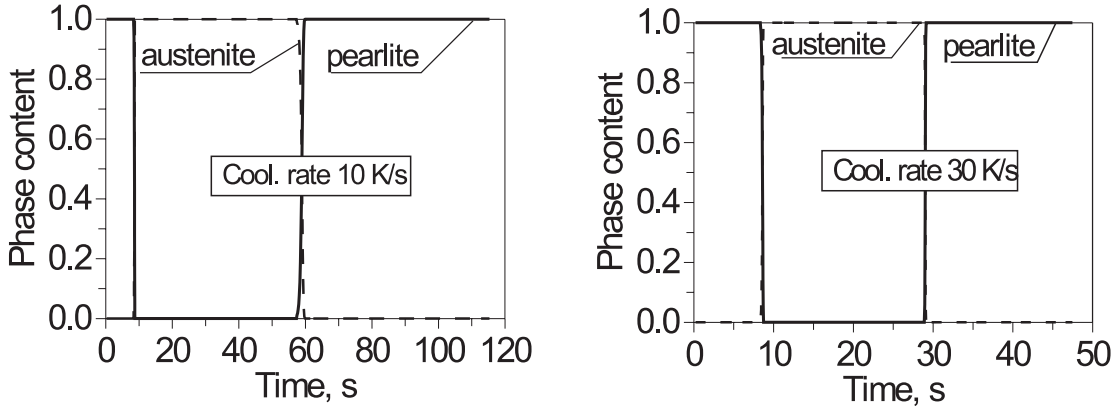

Fig. 3. Kinetics of transformations, cooling rate: a) 10 K/s, b) 30 K/s

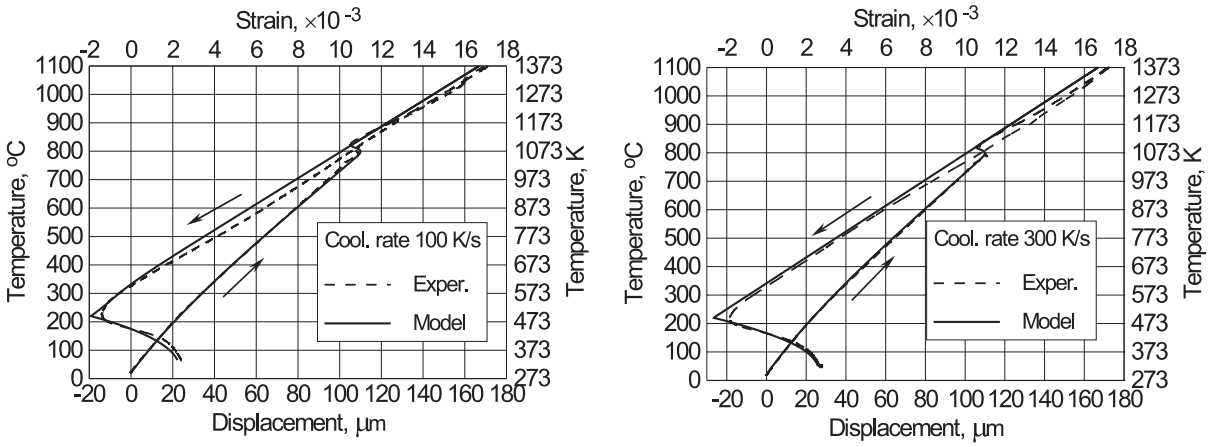

Fig. 4. Experimental and simulated dilatometric curves, cooling rate: a) 100 K/s, b) 300 K/s

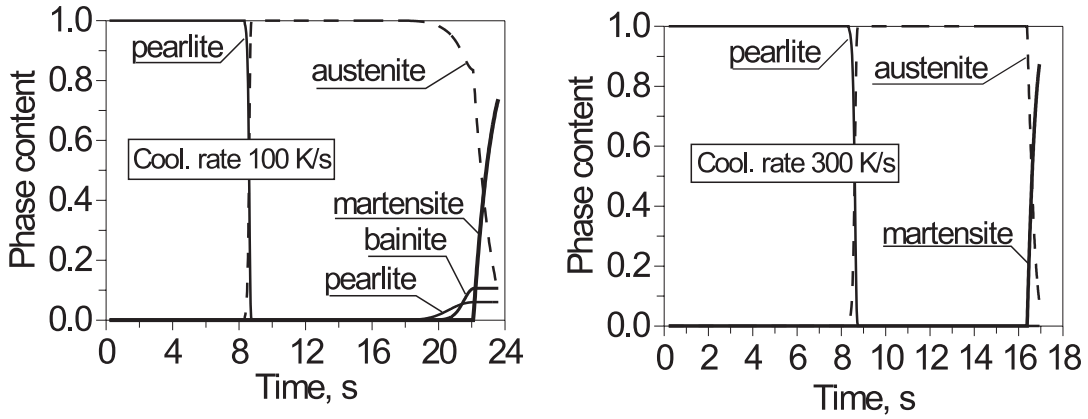

Fig. 5. Kinetics of transformations, cooling rate: a) 100 K/s, b) 300 K/s

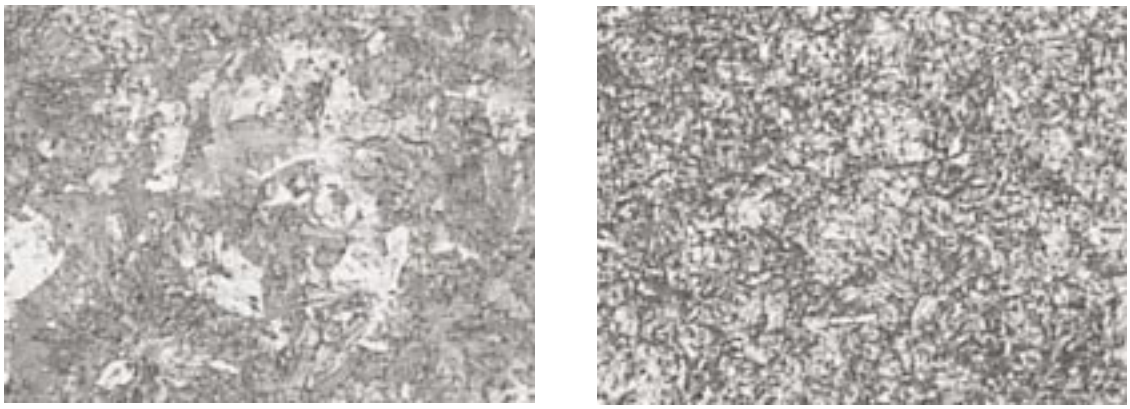

Fig. 6. Microstructure of investigated steel after cooling, zoom ×200, cooling rate: a) 30 K/s, b) 300 K/s

The increment of the isotropic strain provoked by temperature change and phase transformations in the processes of warming and cooling are calculated using formulas [5]:

$$\begin{aligned} d\varepsilon^{Tph} &= \sum_{i=1}^{i=5} \alpha_i \eta_i dT - \varepsilon_\gamma^{ph} d\eta_\gamma, \\ d\varepsilon^{Tph} &= \sum_{i=1}^{i=5} \alpha_i \eta_i dT + \sum_{j=2}^{j=5} \varepsilon_j^{ph} d\eta_j, \end{aligned} \tag{2.5}$$

where: $\alpha_i = \alpha_i(T)$ are thermal expansion coefficients of: austenite, bainite, ferrite, martensite and pearlite, ε_γ^{ph} is an isotropic strain accompanying the conversion of the final structure into austenite, whereas $\varepsilon_j^{ph} = \varepsilon_j^{ph}(T)$ are isotropic strains from phase transformations of: austenite into bainite, ferrite or cementite fraction, martensite or austenite into pearlite respectively. In the steel C80U the cementite fraction is residual ($\leqslant 3\%$) and is a part of the pearlite, so $\delta\eta_3 = 0$ and $\eta_3 = 0$.

These values are set based on experimental research executed on the simulator of thermal cycles. The curves of the CCT diagram are entered to a suitable module used to calculate phase fractions. The curves are supplemented with information on the maximum fraction of a definite phase $\left(\eta_{(\cdot)}^{\%}\right)$. Suitable range determines cooling rates estimated up to the point when the temperature reaches the curve of the transformation start.

Based on comparisons of experimental and simulator dilatometric curves for the examined steel, values of thermal expansion coefficients $(\alpha_{(\cdot)} = \alpha_{(\cdot)}(T))$ and isotropic structural strains $\left(\varepsilon_{(\cdot)}^{ph}\right)$ of each micro-constituents were determined. They equal: 22, 10, 10 and 14.5 ($\times 10^{-6}$) [1/K] and 1.9, 4.5, 8.7 and 1.5 ($\times 10^{-3}$) for austenite, bainite, martensite and pearlite respectively.

Because of the fact that the coefficient of thermal expansion for pearlitic structure of the examined steel depends significantly on the temperature, an approximation of this coefficient using the square function of the form was applied:

$$\alpha_P(T) = -1.2955 \cdot 10^{-11} T^2 + 2.5232 \cdot 10^{-8} T + 3.7193 \cdot 10^{-6}.$$

3. Model of thermal phenomena of the hardening process of steel

In the algorithm of thermal phenomena in the hardening process of steel the conductivity equation is used:

$$\nabla \cdot (\lambda \nabla T(\mathbf{x}, t)) - C_{ef} \frac{\partial T(\mathbf{x}, t)}{\partial t} = -\dot{Q}(\mathbf{x}, t), \tag{3.1}$$

where: $\lambda = \lambda(\mathbf{x})$ is the heat conductivity coefficient [W/(mK)], $C_{ef} = C_{ef}(\mathbf{x})$ is an effective heat capacity [J/(m^{3}K)], which can include the heat of phase transformation $\dot{Q} = \dot{Q}(\mathbf{x}, t)$ is a strength of internal source [W/m^3] (this can also be the phase transformations heat).

Heat of the phase transformation in the solid state can be included in this part of the conductivity equation which represents internal sources $\left(\dot{Q}\right)$ (model with the volumetric internal source), or in the effective heat capacity $\left(C_{ef}\right)$ of this equation (model with the overall heat capacity) [5, 21]. In this work the heat of phase transformations was included in the effective heat capacity assuming that the volumetric fraction of the nascent, k-phase was a function dependent on the temperature $(\eta_k(\mathbf{x}, t) = \eta_k(T(\mathbf{x}, t)))$. When in the equation (3.1) the heat source $\left(\dot{Q}\right)$ represents the heat of transformation phase, then it is assumed that $C_{ef} = C = \rho c$, whereas when the transformation heat is contained in the effective heat capacity then $\dot{Q} = 0$, and the effective heat capacity equals [5]:

$$C_{ef}(T) = \begin{cases} C - \sum\limits_{k} H^{\eta_k} \frac{d\eta_k(T)}{dT}, T \in \left[T_s^k, T_f^k\right] \\ C,\ T \notin \left(T_s^k, T_f^k\right) \end{cases}, \quad (3.2)$$

where: T_s^k and T_f^k are temperatures of the start and the end k -phase transformation, c is heat capacity [J/(kgK)], ρ is density [kg/m^3].

The conductivity equation (3.1) with suitable initial and boundary conditions (Dirichlet, Neumann or Newton) is solved by FEM [21].

4. Model of mechanical phenomena

The equilibrium equation and constitutive relations are used in rate form [5, 15, 22, 23].

$$\begin{gathered} \nabla \circ \dot{\boldsymbol{\sigma}}(\mathbf{x}, t) + \dot{\mathbf{F}}(\mathbf{x}, t) = \mathbf{0}, \quad \dot{\boldsymbol{\sigma}} = \dot{\boldsymbol{\sigma}}^T, \\ \dot{\boldsymbol{\sigma}} = \mathbf{E} \circ \left(\dot{\boldsymbol{\varepsilon}} - \dot{\boldsymbol{\varepsilon}}^{Tph} - \dot{\boldsymbol{\varepsilon}}^{p} - \dot{\boldsymbol{\varepsilon}}^{tp}\right) + \dot{\boldsymbol{E}} \circ \boldsymbol{\varepsilon}^{\mathrm{e}}, \end{gathered} \quad (4.1)$$

where: $\boldsymbol{\sigma} = \boldsymbol{\sigma}\left(\sigma^{\alpha\beta}\right)$ is stress tensor, $\mathbf{F}$ is the vector of volumetric forces, $\mathbf{E} = \mathbf{E}\left(E^{\alpha\beta\gamma\mu}(T, \sum \eta_k)\right)$ is the tensor of material constants dependent on the temperature and the phase composition ($\sum \eta_k$), symbol ($\circ$) represents the internal non-complete product of tensor, $\boldsymbol{\varepsilon}^e = \boldsymbol{\varepsilon}^e\left(\varepsilon^e_{\alpha\beta}\right)$ is a tensor of elastic strains, $\boldsymbol{\varepsilon}^{Tph} = \boldsymbol{\varepsilon}^{Tph}\left(\varepsilon^{Tph}_{\alpha\beta}\right)$ is the tensor of thermal strains and phase transformation (structural strains), $\boldsymbol{\varepsilon}^p = \boldsymbol{\varepsilon}^p\left(\varepsilon^p_{\alpha\beta}\right)$ is the tensor of plastic strains, whereas $\boldsymbol{\varepsilon}^{tp} = \boldsymbol{\varepsilon}^{tp}\left(\varepsilon^{tp}_{\alpha\beta}\right)$ are transformations plasticity.

In order to calculate plastic strains a model of nonisothermal plastic flow with the H u b e r-M i s e s plasticity condition and with the isotropic strengthening is used, where the actual effective stress $Y = Y\left(T, \sum \eta_k, \varepsilon^{\mathrm{p}}_{ef}\right)$ depends on phase composition $\sum \eta_k$ (in the temperature T) and effective strain ε^p_{ef}, ie.:

$$Y\left(T, \sum \eta_k, \varepsilon^{\mathrm{p}}_{ef}\right) = Y_0\left(T, \sum \eta_k\right) + Y_H\left(T, \sum \eta_k, \varepsilon^{\mathrm{p}}_{ef}\right), \quad (4.2)$$

where: $Y_0 = Y_0(T, \sum \eta_k)$ is a yield points of material dependent on the temperature and the phase fraction with no plastic strains, whereas $Y_H = Y_H\left(T, \sum \eta_k, \varepsilon^p_{ef}\right)$ is a surplus of the strain (resulting from the material hardening).

The rate of changes of yield stress equals

$$\dot{Y}\left(T, \sum \eta_k, \varepsilon^p_{ef}\right) = \kappa \dot{\varepsilon}^p_{ef} + H^Y_T \dot{T} + \sum_r H^Y_{\eta_r} \dot{\eta}_r, \quad (4.3)$$

where: $\kappa = \kappa\left(T, \sum \eta_k, \varepsilon^p_{ef}\right)$ is the hardening modulus, $H^Y_T = H^Y_T\left(T, \sum \eta_k, \varepsilon^p_{ef}\right)$ is the thermal softening modulus, $H^Y_{\eta_r} = H^Y_{\eta r}\left(T, \sum \eta_k, \varepsilon^p_{ef}\right)$ is the modulus of structural hardening [2, 3, 5].

In order to estimate transformation plasticity the L e b l o n d model [24] is used. The model is based on the G r e e n w o o d-J o h n s o n mechanism. Transformation plasticity is calculated as follows:

$$\dot{\boldsymbol{\varepsilon}}^{\mathrm{tp}} = \begin{cases} 0, \text{ for } \eta_i \leqslant 0.03, \\ -K_{1i} \frac{\mathbf{S}}{\sigma^Y_1} \ln(\eta_i) \dot{\eta}_i, \quad \text{for } \eta_i \geqslant 0.03, \end{cases} \quad (4.4)$$

where: $K_{1i} = 3\varepsilon^{ph}_{1i}$ are volumetric structural strains when the material is transformed from the initial phase „1" into the i-phase, $\mathbf{S}$ is the deviator of stress tensor.

The equations are solved by means of the FEM [5, 21]. The system of equations used for numerical calculation can be presented as follows:

$$[\mathbf{K}] \left\{\dot{\mathbf{U}}\right\} = \left(\left\{\dot{\mathbf{R}}\right\} + \left\{\dot{\mathbf{t}}^{Tph}\right\} + \left\{\dot{\mathbf{t}}^{ptp}\right\}\right) - \left\{\dot{\mathbf{t}}^{e}\right\}, \quad (4.5)$$

where: $\mathbf{K}$ is the element stiffness matrix, $\dot{\mathbf{U}}$ is the vector of nodal displacement, $\dot{\mathbf{t}}^{Tph}$ is the vector of nodal forces resulting from thermal strains and structural strains, $\dot{\mathbf{t}}^{e}$ is the vector of nodal forces resulting from the value change of Y o u n g's modulus dependent on the temperature, $\dot{\mathbf{R}}$ is the vector of nodal forces resulting from the boundary load and the inertial forces load, and $\dot{\mathbf{t}}^{ptp}$ is the vector of nodal forces n resulting from plastic strains and transformation plasticity.

The rate vectors of loads in the brackets are calculated only once in the increment of the load, whereas the vector $\dot{\mathbf{t}}^{ptp}$ is modified in the iterative process. The modified Newton-Raphson algorithm [25] was used.

The obtained model of the hardening process of steel C80U consists of three related parts: thermal part, phase transformations part and stress part. The model gives the possibility to simulate the progressive and volumetric hardening process for any geometries (task 2D, including axisymetrical tasks). The in-house program was developed by implementing the model in the programming environment Delphi.

5. Example of calculations

Numerical simulations of hardening of the elements made of the carbon tool steel C80U were performed. The thermophysical coefficients λ and C_v were assumed as constants: 34 [W/(mK)], and 5432×10^3 [J/(m^{3}K)]. These are the average values calculated on the basis of

the data in the work [14]. Transformation heats of phase transformation equal ([J/m^3]) [26, 27]:

$$\Delta H_{\gamma\to P} = 800.6\cdot 10^6, \Delta H_{\gamma\to B} = 314\cdot 10^6, \quad \Delta H_{\gamma\to M} = 628\cdot 10^6. \tag{5.1}$$

Young's and tangential moduli (E and E^t) were dependent on temperature, whereas the yield stress (Y) was dependent on temperature and phase composition. These values were approximated with the use of square functions using the following assumptions based on the work [4]: Young's and tangential moduli 2×10^5 and 2×10^4 [MPa], yield points 150, 480, 950 and 320 [MPa] for austenite, bainite, martensite and pearlite, respectively, in the temperature 300 K. In the temperature 1700 K Young's modulus and tangential modulus equalled 100 and 10 [MPa], respectively, whereas yield points equalled 5 [MPa].

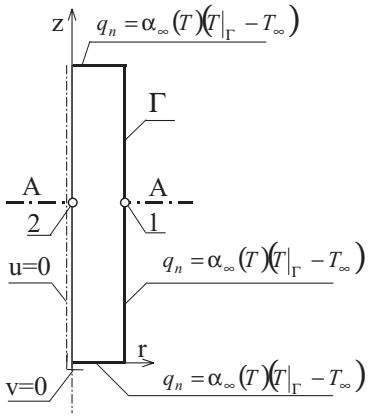

Fig. 7. The scheme of the system and boundary conditions

The axisimmetrical object with the following size ϕ30×60 mm (Fig. 6–7) underwent hardening simulation. After heating it had an even temperature equalling 1100 K, and the output microstructure was austenite. The cooling was modelled with the Newton condition. The temperature of the cooling medium equalled T_∞ = 300 K. The dependence of the heat transfer coefficient $\alpha_\infty = \alpha_\infty$(T) (from the external surface „γ") on the temperature was presented by means of square and linear functions (Fig. 8).

Distributions of the fractions in the microstructure after hardening of the object cooled in water and fluid layer are presented in Figures 9–11.

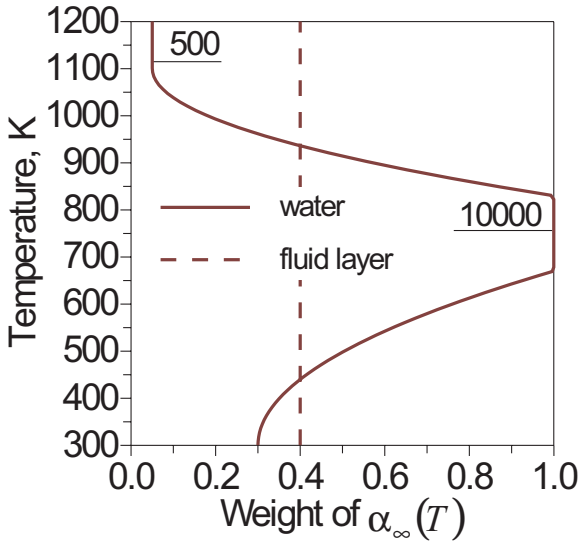

Fig. 8. Plot of functions approximating $\alpha = \alpha$(T) and their extreme values [W/(m^{2}K)]

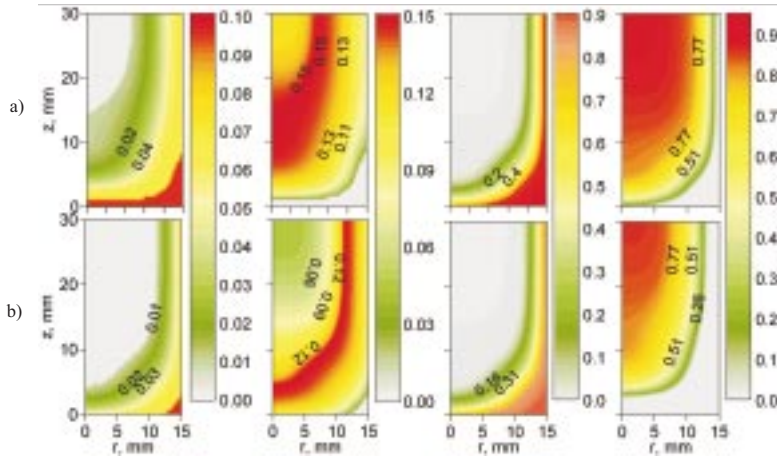

Fig. 9. Phase fractions after hardening, in turn: retained austenite, bainite, martensite and pearlite. a) cooling in water, b) cooling in fluid layer

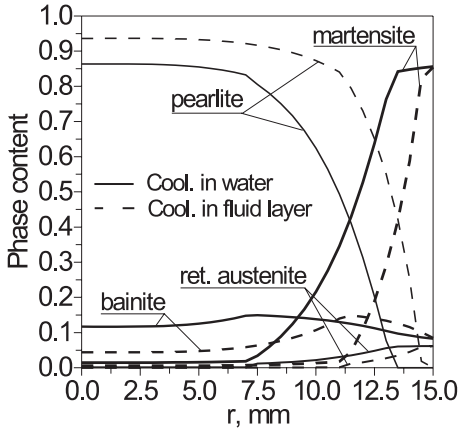

Fig. 10. Hardened zones in central cross section (A-A, Fig. 7)

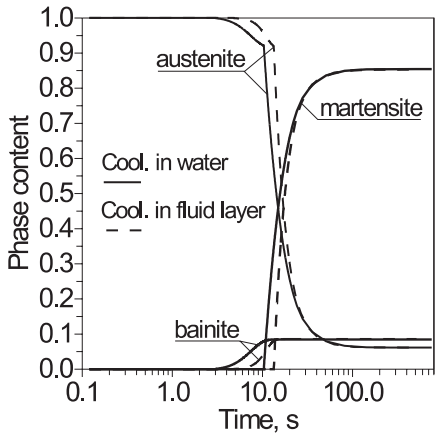

Fig. 11. The kinetics of transformation in the superficial point 1 of the element (Fig. 7)

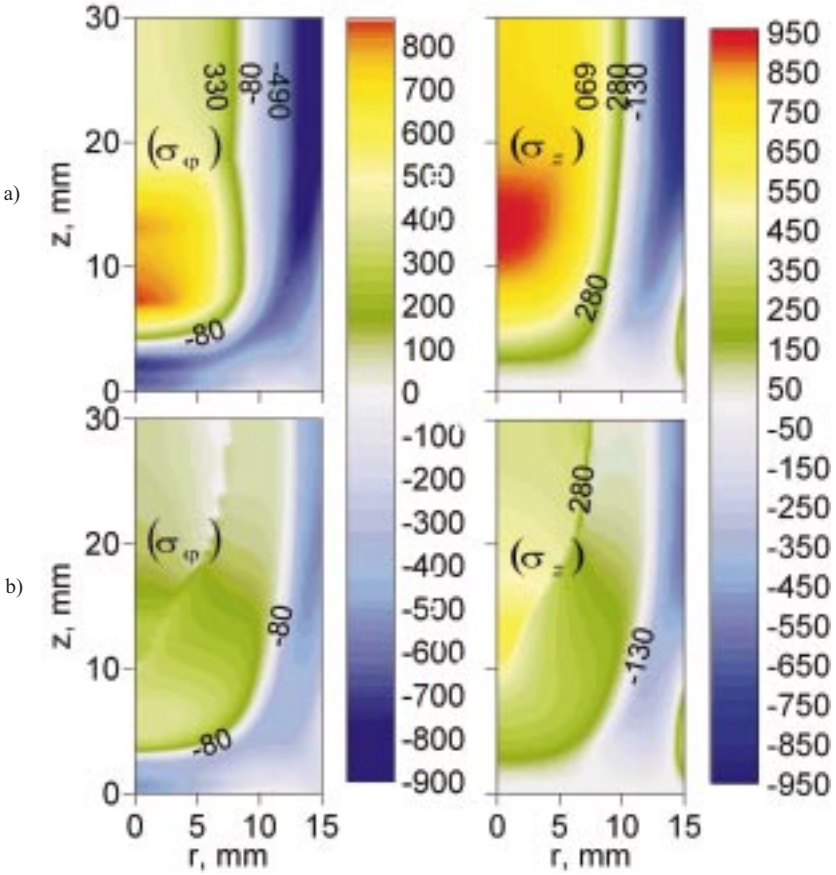

Fig. 12. Distributions of residual stress σ_φ and σ_z [MPa] after hardening in water. a) $\boldsymbol{\varepsilon}^{tp} = \mathbf{0}$, b) $\boldsymbol{\varepsilon}^{tp} \neq \mathbf{0}$

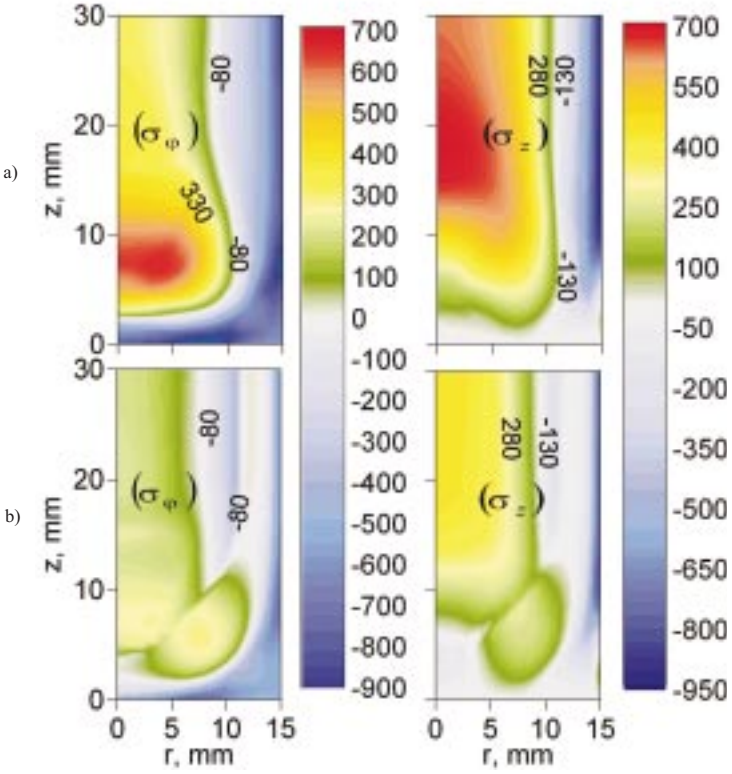

Fig. 13. Distributions of residual stress σ_φ and σ_z [MPa] after hardening in fluid layer. a) $\boldsymbol{\varepsilon}^{tp} = \mathbf{0}$, b) $\boldsymbol{\varepsilon}^{tp} \neq \mathbf{0}$

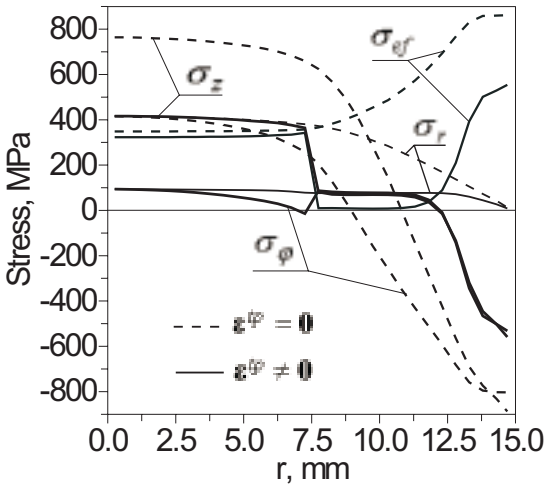

Fig. 14. Residual stresses in central cross section (A-A, Fig. 7) without and with considering transformations plasticity (cooling in water)

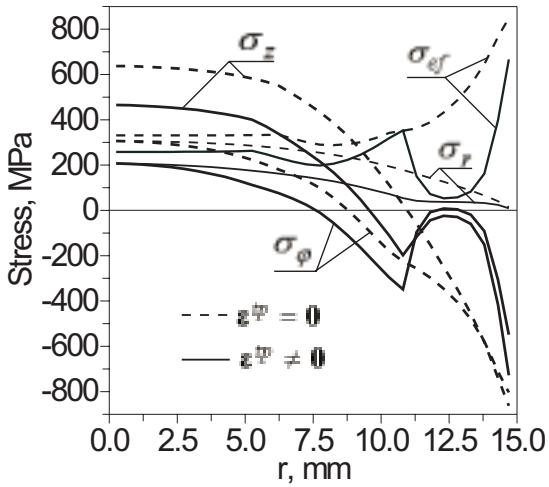

Fig. 15. Residual stresses in central cross section (A-A, Fig. 7) without and with considering transformations plasticity (cooling in fluid layer)

Exemplary residual stress distributions with and without transformation plasticity: ($\varepsilon^{tp} = \mathbf{0}$) and ($\varepsilon^{tp} \neq \mathbf{0}$) respectively are presented in Figures 12–15.

6. Conclusions

The results of the verification of the phase transformations model are satisfactory and confirm the correctness of the designed model of phase transformations for the carbon tool steel (Figs. 2 and 4). Having analysed the results of the object hardening simulation after full austenitizations it can be noticed that the hardened layer is comparable to the one obtained after deep inductive heating (Figs. 9 and 10) [1, 3].

However when cooling in the fluid layer is performed more superficial deposition of the martensite is

obtained and a slightly bigger deposition of the bainite in superficial layers can be observed.

Stress distributions after such hardening are advantageous, both in case of cooling in water, as well as cooling in the fluid layer (Figs. 12—15). More regular distributions of the stresses are obtained after cooling in the fluid layer (Figs. 13 and 15). However extreme values of these stresses are comparable.

Inclusion of transformation plasticity has a significant influence on distributions and extreme values of stresses in the simulation of the hardening. The deposition of negative circumferential and axial strains is more superficial, and their extreme values are lower when these strains are taken into account (Figs. 14 and 15). It can be claimed that in the numerical simulation of such hardening the fact that transformation plasticity is included in the model of mechanical phenomena brings about significant changes in obtained results. These changes encompass smoothing of strain fields and decrease in their peaks. It appears to be highly right.

REFERENCES

[1] A.J. Fletcher, Thermal Stress and Strain Generation in Heat Treatment, Elsevier, London (1989).

[2] A. Bokota, S. Iskierka, Effect of phase transformation on stress states in surface layer of laser hardened carbon steel, ISIJ International **36(11)**, 1383-1391 (1996).

[3] B. Raniecki, A. Bokota, S. Iskierka, R. Parkitny, Problem of determination of transient and residual stresses in a cylinder under progressive induction hardening, The 3rd International Conference On Quenching And Control Of Distortion, Prage, Czech Republic, Published by ASM International, 473-484 (1999).

[4] M. Coret, A. Combescure, A mesomodel for the numerical simulation of the multiphasic behavior of materials under anisothermal loading (application to two low-carbon steels), International Journal of Mechanical Sciences **44**, 1947-1963 (2002).

[5] T. Domański, Numerical modelling of surface hardening elements of steel. PhD Thesis, Częstochowa (2005). (in polish)

[6] A. Bokota, T. Domański, The numerical model of progressive hardening of elements machine made of tool steel. Informatyka w Technologii Metali, Materiały XII Konferencji, 65-72 (2005). (in polish)

[7] K.J. Lee, Characteristics of heat generation during transformation in carbon steel. Scripta Materialia **40**, 735-742 (1999).

[8] W. Piekarska, Phase transformation in HAZ of welded joints made by laser welding with preaheating. Mathematical model. Procedings of Second International Conference "Mathematical modelling and information technologies in welding and related processes", Katsiveli, Crimea, Ukraine, 220-224 (2004). (in russien).

[9] W. Piekarska, The numerical analysis of phase transformation in the welded high strength steel, Inżynieria Materiałowa **24**, 524-526 (2005). (in polish)

[10] M. Pietrzyk, R. Kuziak, Coupling the Thermal-Mechanical Finite-Element Approach with Phase Transformation Model for Low Carbon Steels, Mat. 2. Konf. ESAFORM, ed., J. Covas, Guimaraes, 525-528 (1999).

[11] M. Pietrzyk, Through-process modelling of microstructure evolution in hot forming of steels, Journal of Materials Processing Technology **125-126**, 53-62 (2002).

[12] J. Rońda, G.J. Oliver, Consistent thermo-mechanical-metallurgical model of weldet steel with unified approach to derivation of phase evolution laws and transformation-induced plasticity, Computer Methods Applied mechanics and engineering **189**, 361-417 (2000).

[13] M. Cherkaoui, M. Berveiller, H. Sabar, Micromechanical modeling of martensitic transformation induced plasticity (TRIP) in austenitic single crystals, International Journal of Plasticity **14**, 7, 597-626 (1998).

[14] M. Coret, S. Calloch, A. Combescure, Experimental study of the phase transformation plasticity of 16MND5 low carbon steel induced by proportional and nonproportional biaxial loading paths. European Journal of Mechanics A/Solids **23**, 823-842 (2004).

[15] R.B. Pęcherski, Finite deformation plasticity with strain induced anisotropy and shear banding. Journal of Materials Processing Technology **60**, 35-44 (1996).

[16] H.C. Gür, E.A. Tekkaya, Numerical investigation of non-homogeneous plastic deformation in quenching process. Materials Science and Engineering **A319-321**, 164-169 (2001).

[17] J. Jasiński, Influence of fluidized bed on diffusional processes of saturation of steel surface layer. Seria: Inżynieria Materiałowa Nr 6, Wydawnictwo WIPMiFS, Częstochowa (2003).

[18] D.P. Koistinen, R.E. Marburger, A General Equation for Austenite – Martensite Transformation in Pure Carbon Steels, Acta Metallurgica **7**, 59-60 (1959).

[19] M. Białecki, Characteristic of steels, seria F, tom I, Wydawnictwo Śląsk **108-129**, 155-179 (1987). (in polish)

[20] A. Bokota, T. Domański, W. Zalecki, The numerical model of phase transformations in carbon tool steels, Archives of Foundry **22**, 75-82 (2006). (in polish)

[21] O.C. Zienkiewicz, R.L. Taylor, The finite element method, Butterworth-Heinemann, Fifth edition **1,2,3** (2000).

[22] J.M. Cabrera, J. Ponce, J.M. Prado, Modeling thermomechanical processing of austenite, Journal of Materials Processing Technology **143-144**, 403-409 (2003).

[23] R.B. Pęcherski, Macroscopic effects of micro-shear banding in plasticity of metals. Acta Mech. **131**, 203-224 (1998).

[24] L. Taleb, F. Sidoroff, A micromechanical modelling of the Greenwood-Johnson mechanism in transformation induced plasticity, International Journal of Plasticity **19**, 1821-1842 (2003).

[25] S. Caddemi, J.B. Martin, Convergence of the Newton-Raphson algorithm in elastic-plastic incremental analysis, Int. J. Numer. Meth. Eng. **31**, 177-191 (1991).

[26] S. Serejzadeh, Modeling of temperature history and phase transformation during cooling of steel, Journal of Materials Processing Technology **146**, 311-317 (2004).

[27] E.P. Silva, P.M.C.L. Pacheco, M.A. Savi, On the thermo-mechanical coupling in austenite-martensite phase transformation related to the quenching process, International Journal of Solids and Structures **41**, 1139-1155 (2004).

Received: 10 March 2007.